

# Star Elimination as a Means of Resident Space Object Identification for Space Situational Awareness

Evan Pavetto-Stewart<sup>1</sup> and Thomas Alan Lovell<sup>2</sup>  
*Embry-Riddle Aeronautical University, Daytona Beach FL*

**Accurately identifying resident space objects within optical space imagery poses a key challenge in the realm of Space Situational Awareness. For unresolved imagery, the primary issue is distinguishing RSOs from stars and other objects (or aberrations) that may be present. In this paper the authors will explore the RSO identification process in optical scenarios, particularly the process of eliminating stars from image data, to facilitate the frame-to-frame association of data points belonging to RSOs. Different star elimination strategies are developed and tested, with an emphasis on their adaptive use for autonomous applications.**

## I. Introduction

A fundamental tenet of Space Situational Awareness (SSA) is to properly identify resident space objects (RSOs) within unresolved optical space imagery. This subsequently allows the directional data, i.e. right ascension (RA) and declination (Dec), for each RSO to be processed resulting in an estimate of each RSO's orbit. The emphasis here will be on developing an algorithm to identify Earth-orbiting RSOs that can be accomplished autonomously onboard a spacecraft.

In order to distinguish RSOs from the star field, a suggested practice is to perform multi-frame image collects and identify RSOs based on how the scene changes from frame to frame.[1] Two common modes of imaging are described as follows:

- Inertial stare mode: Here the camera's attitude is controlled so as to remain inertially fixed. Ideally, stars will remain stationary in the camera's field of view, but RSOs will move over time. For a long enough exposure time, the RSO will exhibit streaking in the image (see Figure 1).
- Orbit-following mode: Here the camera's attitude is controlled so as to follow an RSO whose orbit is known with at least some degree of accuracy. Ideally, the RSO will remain stationary in the camera's field of view, but stars will move over time (again, streaking for long enough exposure times) (see Figure 2).

In order to operate on these and other types of collects, an RSO identification (RSOID) algorithm must be robustly designed, firstly to distinguish actual objects in the images from false objects (i.e. collections of "noisy" pixels) and secondly, to distinguish RSOs from stars or other celestial objects.

---

<sup>1</sup> Master's Student, Aerospace Engineering Department, AIAA Student Member.

<sup>2</sup> Professor, Aerospace Engineering Department, AIAA Associate Fellow.



**Figure 1 Unresolved image taken in inertial stare mode with captured RSO evident in upper right.**



**Figure 2 Unresolved image taken in orbit-following mode with captured RSO circled.**

## II. RSOID Methodology

Previous work [2-4] developed an initial version of an RSO identification (RSOID) algorithm that was limited in the types of images and RSOs that could be processed. The algorithm consists of the following interdisciplinary steps:

- Edge detection for each image in the collect, to determine the boundary between each set of illuminated pixels and the blackness of space; this reduces each image to numerous segmented “objects” (actually point spread functions)
- Centroiding for each image in the collect, to localize each object in the camera frame based on x,y- pixel coordinates
- Registration (or “plate solving”) of each image, to determine the inertial pointing of the camera and thereby convert the  $x, y$  coordinates of each centroid in the camera frame to inertial coordinates (i.e., RA and Dec)
- Star elimination, to remove all centroids identified as belonging to a star
- Object association, to confirm the existence of each RSO tracklet (i.e. collection of RA/Dec data points) by performing linear regression on sets of remaining centroids across the collect

This process is illustrated in Figure 3. In order to gauge the algorithm’s performance, it is instructive to examine the output of each step above. Toward this end, the following two figures illustrate the output of plate solving and star elimination for an example multi-frame image collect. Figure 4 represents an overlay of all centroids detected across all frames and displayed as RA vs Dec, with the centroids of the first frame appearing as blue circles, the centroids of the last frame appearing as red circles, and the remaining frames utilizing a linear spread across the color spectrum. Note that the vast majority of centroids appear red, with few centroids of any other color. In fact, most of the circles represent a closely spaced “cluster” of circles, representing the occurrence of a particular star in all (or most) frames of the collect. Thus, overall there are likely a few thousand centroids depicted. Figure 5 is the same plot after executing the star elimination step of the process. Among the comparatively few centroids that remain, the frame-to-frame motion of an RSO can be seen near the center of the plot, appearing as a quasi-linear path from left to right.

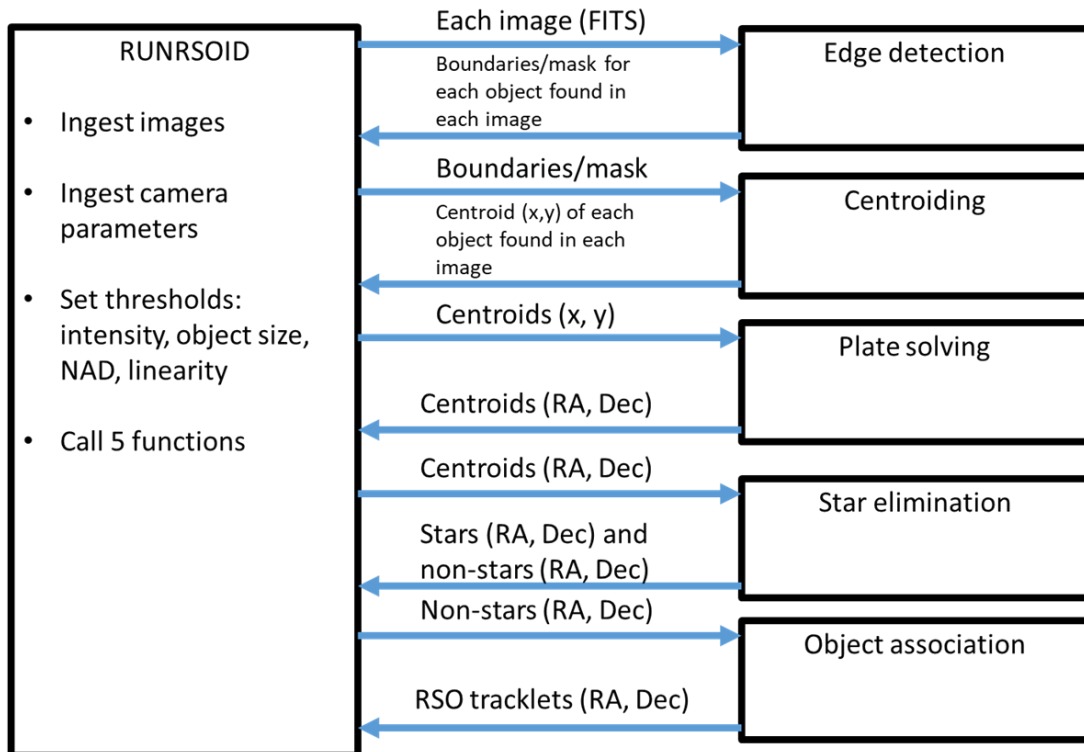
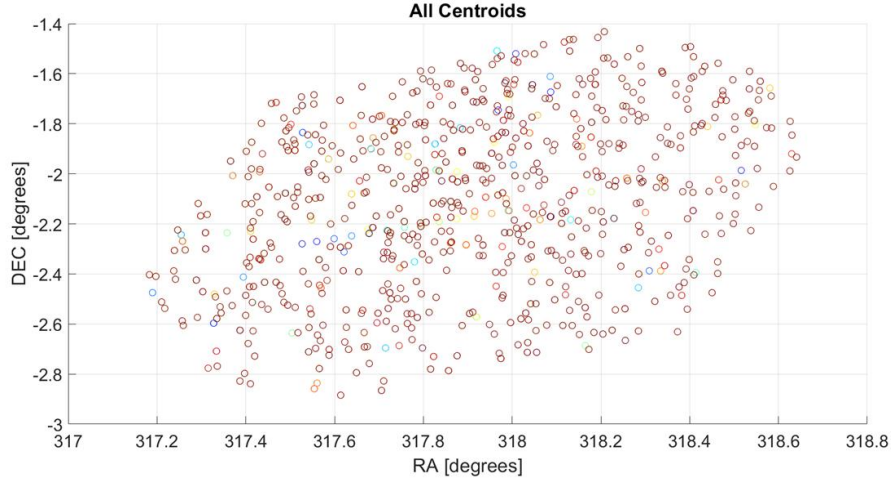
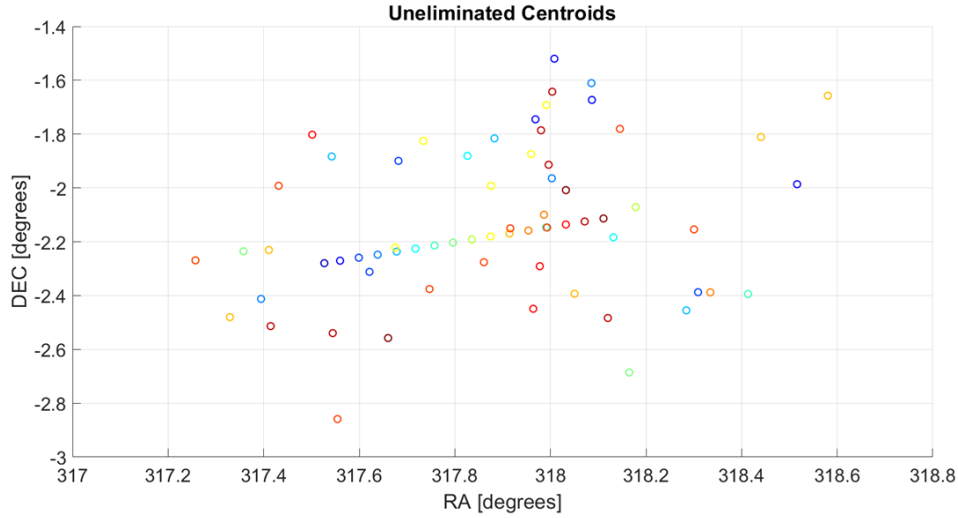


Figure 3 Flow chart describing the RSOID process.



**Figure 4** For an example collect, aggregation of all centroids from each frame superimposed together.



**Figure 5** Centroids remaining in the collect after star elimination.

### III. Star Elimination

In order to improve the algorithm’s performance, recent efforts have focused on refining the various steps in the algorithm’s process.[5] In the present paper, the authors investigate the star elimination step of the process, the effects of which can be visually ascertained from Figures 4 and 5 below. Ideally, this step would remove all stars from the frames of a collect, such that the only centroids to remain would be RSOs and perhaps false objects generated by collections of contiguous “noisy” pixels that were misconstrued as objects during the edge detection phase. This would maximize the probability of success in the final phase, object association, such that each set of RA/Dec data points belonging to the same RSO would be associated together into tracklets, which are in fact the desired output of the algorithm. Given this goal, a key metric in any star elimination strategy is termed the “norm angular difference” between two centroids in different frames of a collect and is defined as follows:

$$NAD = \sqrt{(RA_2 - RA_1)^2 + (Dec_2 - Dec_1)^2} \quad (1)$$

Where  $(RA_1, Dec_1)$  and  $(RA_2, Dec_2)$  are the RA and Dec locations of the two centroids. If we assume that the RA and Dec of each star in the universe remains constant over the course of a collect (i.e. a few minutes at most), then ideally the centroid representing a particular star in Frame 1 of a collect would lie at the same RA and Dec as the centroid representing that star in Frame 2 of the collect, as well as in Frame 3, etc. This will not be the case. Rather, each occurrence of a particular star will lie at a slightly different RA and Dec from one frame to the next. The design of

any star elimination capability will be based largely on how closely clustered these occurrences are (in terms of NAD) throughout the different frames of the collect.

It then stands to reason that a threshold on NAD can be defined such that, if two centroids from different frames are closer than the threshold (i.e. their NAD is less than the threshold value), they belong to the same star. This allows the two centroids to be eliminated going forward. What follows is a description of two candidate star elimination strategies, both of which rely on such a threshold.

#### **A. Clustering**

This strategy is based on the amount by which the RA and Dec location of a particular star (or in fact the centroid representing that star) can vary (in terms of NAD) from frame to frame in a collect. It is in fact this strategy that produced the results of Figure 5 above. For a particular centroid  $\alpha$  in the collect, the NAD is calculated between  $\alpha$  and each centroid not in the same frame as  $\alpha$ . If one of those NADs is less than the star elimination NAD threshold, then  $\alpha$  is labeled as a star. In other words, if the NAD between a centroid and its nearest neighbor is less than the NAD threshold, that centroid is labeled as a star.

#### **B. Catalog comparison**

This strategy involves comparing the RA/Dec value of each centroid in a collect with the RA/Dec values in a star catalog. This too would involve the threshold defined above, in that any centroid that is within the NAD threshold of a catalogued star would in fact be labeled as a star. The authors possess both the Tycho-2 catalog [6] (approx. 2.5 million stars) and a portion of the Gaia catalog [7] (approx. 151 million stars, here referred to as “Gaia LITE”), both of which will be involved in the results of the next section.

### **IV. Results on Real Image Data**

Numerous collects of unresolved space imagery have been obtained via an optical sensor configuration available through the authors’ university. This consists of a Celestron RASA 11 inch telescope with an ASI 1600mm monochrome CMOS camera mounted on a Celestron CGE Pro mount (see Figure 6). The field of view for this configuration is approximately  $1.5^\circ \times 1.5^\circ$ . In this section, two particular collects are emphasized. They are a 31-frame inertial stare collect spanning 41 seconds and a 12-frame object-following collect spanning 23 seconds.



**Figure 6 Optical equipment for collection of real imagery.**

### A. Analysis of Inertial Stare Collect

First emphasizing the inertial stare collect, we see from Table 1 that there are approximately 200 centroids in each frame. Figure 7 is an overlay of all centroids in the collect, displayed in the same fashion as Figure 4. While the motion of two RSOs is already visually apparent here, the ability of the algorithm to identify them is dependent on eliminating as many of the non-RSO centroids (most of which are stars) as possible. Figure 8 is the same plot after implementing star elimination based on clustering, as described in the previous section, with the NAD threshold set to  $0.005^\circ$ . Note that only a small portion of the total 6,000+ centroids remain in the figure, including the centroids pertaining to the RSOs. These remaining centroids will be referred to as “non-stars.” It should be noted that a portion of the longer RSO tracklet is inadvertently eliminated during this step, as highlighted in Figure 9. This is likely because the RSO transits in front of a star about halfway through the collect. This can confuse the edge detection and centroiding steps of the process, which in turn can have a detrimental effect during star elimination.

**Table 1** Number of centroids, Tycho-2 stars, and Gaia LITE stars contained in the inertial stare collect.

Frame #	# of centroids	# of Tycho2 stars	# of Gaia LITE stars	Frame #	# of centroids	# of Tycho2 stars	# of Gaia LITE stars
1	210	103	3221	16	204	103	3157
2	211	103	3220	17	207	103	3261
3	209	103	3157	18	208	103	3157
4	216	103	3220	19	213	103	3156
5	208	103	3156	20	206	103	3221
6	214	103	3158	21	209	103	3156
7	205	103	3156	22	204	103	3156
8	208	103	3155	23	213	103	3156
9	208	103	3156	24	206	103	3159
10	205	103	3157	25	208	103	3221
11	206	103	3262	26	206	103	3260
12	206	103	3263	27	214	103	3156
13	209	103	3221	28	210	103	3157
14	202	103	3221	29	205	103	3156
15	206	103	3261	30	207	103	3156
				31	212	103	3155

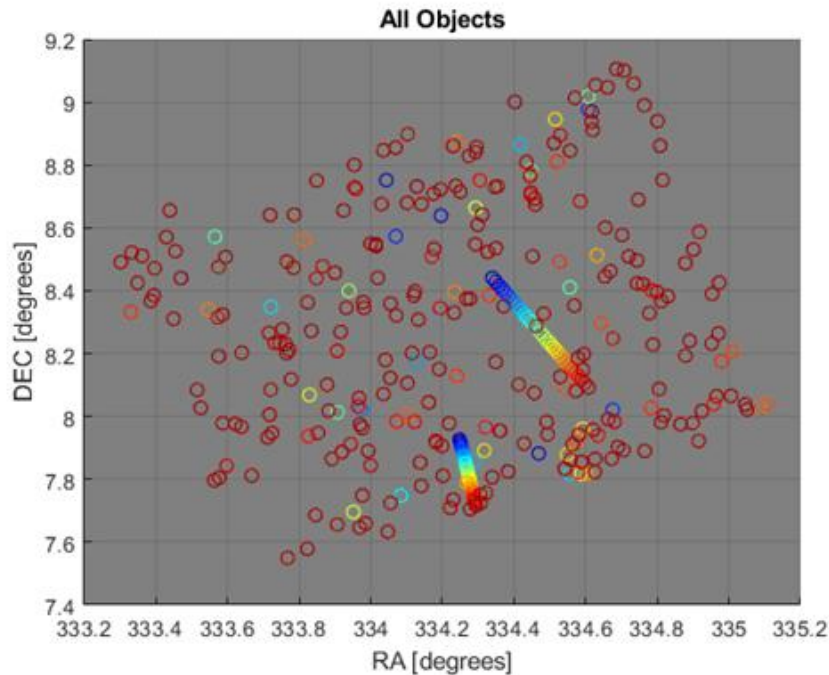


**Figure 7** Aggregation of all centroids from each frame superimposed together, for the inertial stare collect.

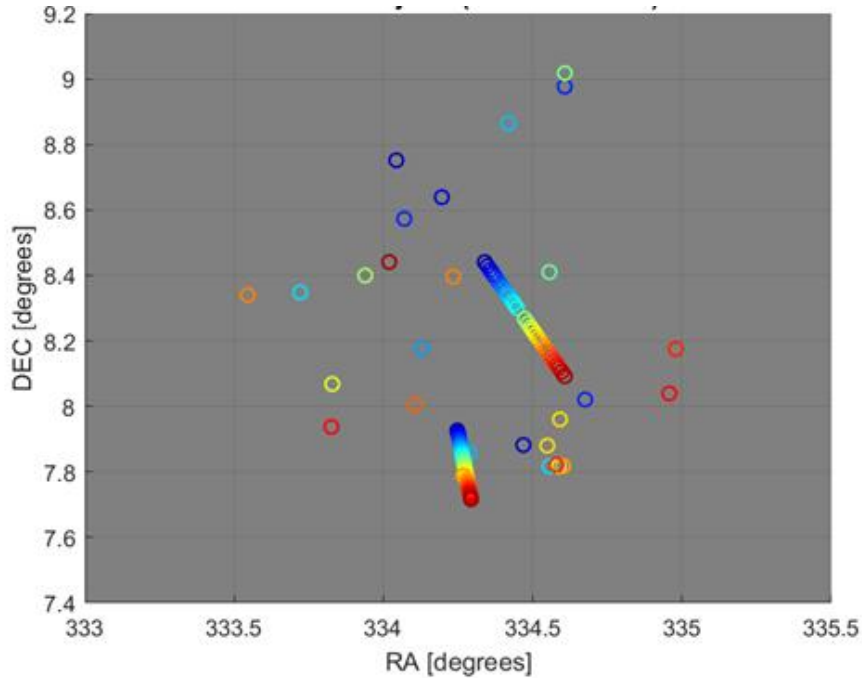


**Figure 8** Centroids remaining in inertial stare collect (i.e. “non-stars”) after star elimination based on clustering (NAD threshold =  $0.005^\circ$ ).

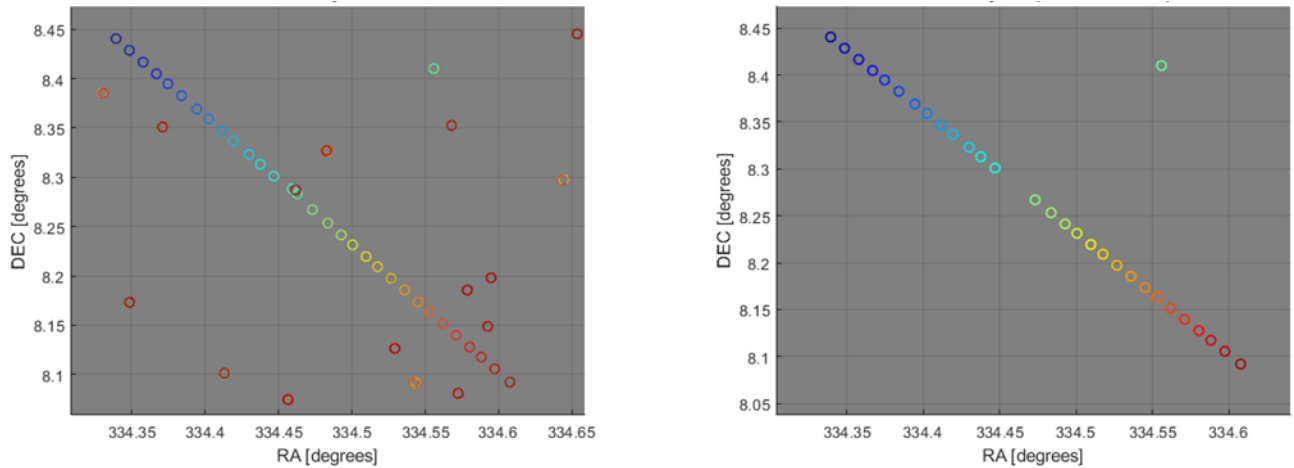


**Figure 9** Longer RSO tracklet in inertial stare collect before (left) and after (right) star elimination.

The authors then considered the implementation of star elimination for the inertial stare collect via catalog comparison rather than clustering. Table 1 compares the number of centroids in each frame with the number of Tycho-2 stars and number of Gaia LITE stars within the specific RA and Dec range of each frame. We conclude from this table that while Tycho-2, at best, could eliminate about half the centroids in each collect, Gaia LITE could potentially eliminate all of them. Therefore the authors proceeded to implement star elimination via comparison with the Gaia LITE catalog. That is, for each centroid in each frame, the NAD was calculated between that centroid and each Gaia LITE star expected to appear in that frame, and any centroid whose Gaia LITE nearest neighbor was closer than the threshold was labeled a star. For example, for each centroid in Frame 1, its nearest neighbor among the 3221 Gaia LITE stars was calculated, and each centroid with a nearest neighbor within the NAD threshold was labeled a star and eliminated. Figure 10 is the result of this, with the NAD threshold again set to  $0.005^\circ$ . Again the vast majority of stars has been eliminated, and in this case the number of non-stars remaining is noticeably less than those eliminated via the clustering technique above.

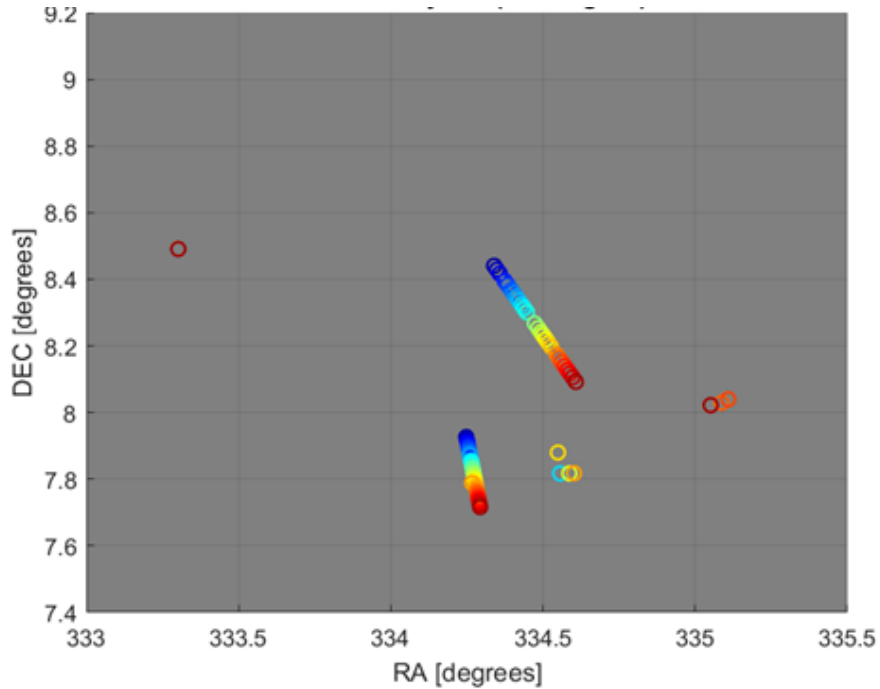


**Figure 10 Centroids in inertial stare collect after star elimination based on comparison with the Gaia LITE catalog (NAD threshold = 0.005°).**

Examining Figures 8 and 10, it is noted that, for this choice of NAD threshold, some centroids eliminated via catalog comparison are not eliminated via clustering, and vice versa. Therefore the authors explored the use of both techniques implemented consecutively. That is, first star elimination via catalog comparison was implemented on all centroids from the inertial stare collect, then star elimination via clustering was implemented on the non-stars resulting from the catalog comparison stage. Figure 11 is the result of this, with the NAD threshold remaining at 0.005° for both stages of the process. Inspection of this figure reveals that, along with the RSO centroids, only 5 other centroids remain uneliminated.

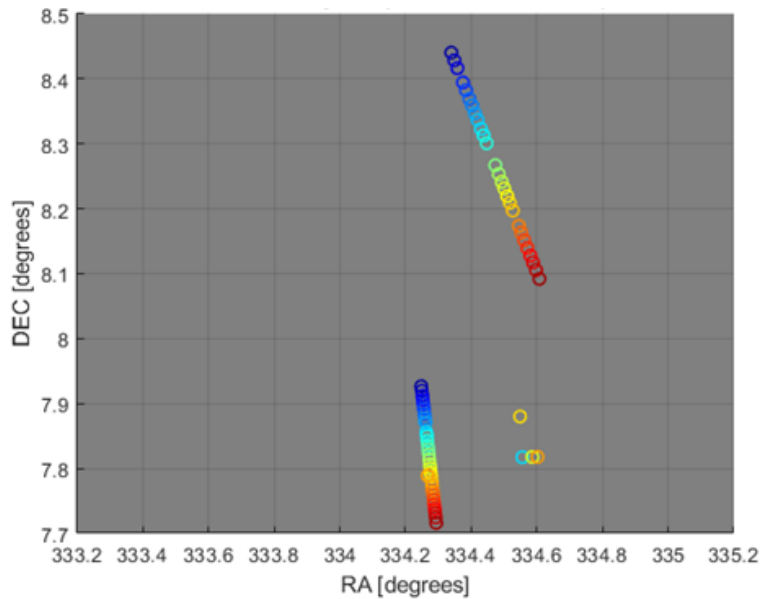


**Figure 11 Centroids in inertial stare collect after implementing Gaia LITE comparison followed by clustering (NAD threshold = 0.005°).**

## B. Analysis of Object-Following Collect

This analysis was then repeated with the object-following collect mentioned above. This collect represents a stare at a portion of the Geostationary (GEO) belt, wherein 6 GEO RSOs are captured. Table 2 lists the number of centroids, Tycho-2 stars, and Gaia LITE stars associated with each frame. Figure 12 shows all centroids in the collect, Figure 13 shows the result of star elimination based on clustering alone, Figure 14 shows the result of star elimination based on catalog comparison, and Figure 15 shows the result of both techniques used consecutively. In all cases, the NAD threshold was set to  $0.005^\circ$ , as it was for the analysis of the inertial stare collect. Again this eliminates the vast majority of stars from the collect, but as before, upon close inspection we see that some of the centroids belonging to RSOs have been eliminated as well, for reasons similar to what was pointed out in Figure 9. This can likely be remedied by a more judicious choice of NAD threshold. Whereas here a blanket value has been chosen for all of the results, the “best” value likely will vary and will depend on the nature of the collect. This relates to a future goal of this effort and is described below.

**Table 2 Number of centroids, Tycho-2 stars, and Gaia LITE stars contained in the object-following collect.**

Frame #	# of centroids	# of Tycho2 stars	# of Gaia LITE stars
1	396	107	6820
2	351	107	6950
3	380	106	6867
4	409	106	6869
5	341	104	6868
6	403	108	6088
7	394	108	6815
8	397	108	6816
9	407	109	6897
10	376	109	6892
11	404	109	6898
12	379	109	6895

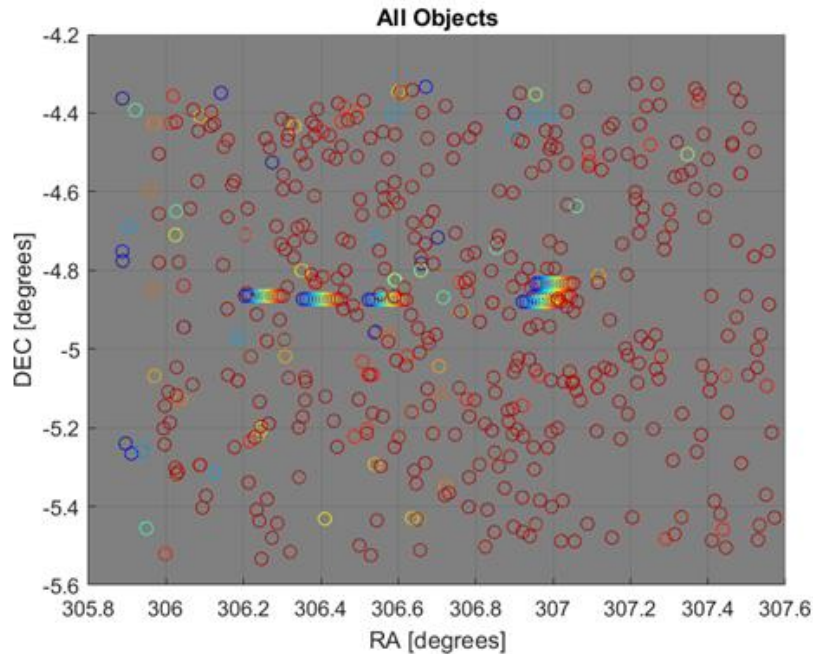


**Figure 12 Aggregation of all centroids from each frame superimposed together, for the object-following collect.**

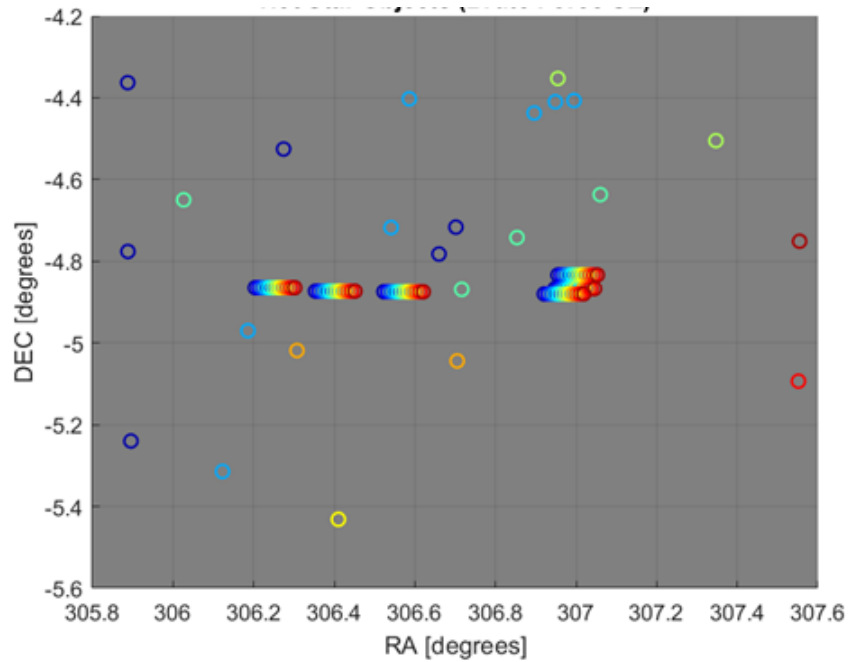


Figure 13 Centroids remaining in object-following collect after star elimination based on clustering (NAD threshold =  $0.005^\circ$ ).

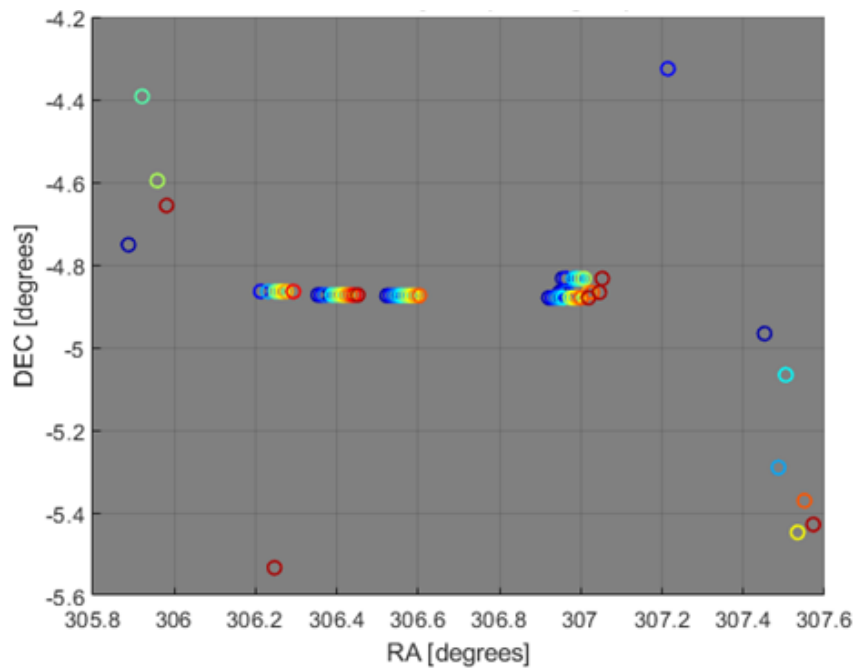
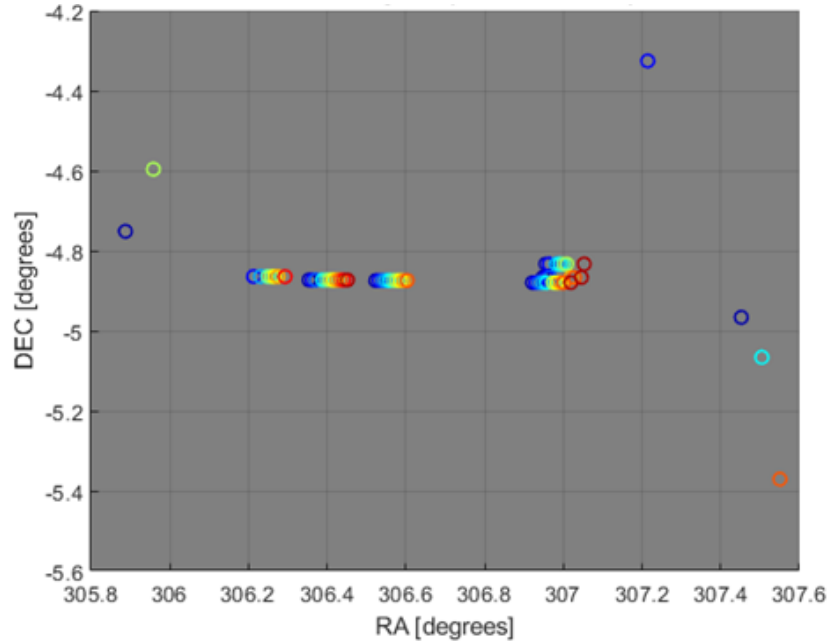


Figure 14 Centroids in object-following collect after star elimination based on comparison with the Gaia LITE catalog (NAD threshold =  $0.005^\circ$ ).



**Figure 15 Centroids in object-following collect after implementing Gaia LITE comparison followed by clustering (NAD threshold =  $0.005^\circ$ ).**

## V. Conclusion and Future Work

This paper has showcased a portion of a resident space object identification algorithm known as star elimination. The premise of the algorithm is to process a multi-frame collect of unresolved space imagery in order to identify earth orbiting space objects among the celestial objects (e.g. stars). Once all objects in the collect have been located and centroided, the star elimination phase removes as many stars from consideration as possible, so that space object data points can be associated together for later use, such as orbit determination of each object. Here multiple star elimination strategies have been laid out, with results shown on collects of real space imagery. The method is effective at removing the vast majority of stars, but occasionally at the expense of removing some of the resident space object centroids as well. Future work will involve investigating the sensitivity of the results to the choice of “norm angular difference” threshold, as well as development of an adaptive threshold scheme based on the statistics (e.g. mean and standard deviation) of norm angular difference between and among clusters of centroids. Increasing the reliability of this algorithm will aid in collision avoidance and trajectory planning in space situational awareness applications.

## References

- [1] Zuehlke, D., “Space Image Processing and Orbit Estimation Using Small Aperture Optical Systems,” Embry-Riddle Aeronautical University, PhD Dissertation, Apr. 2023.
- [2] Lovell, T.A., Zuehlke, D., and Henderson, T., “Processing of Space Object Data from Optical Observers for Space Domain Awareness,” 2021 IEEE Aerospace Conference (50100), IEEE, Mar. 2021, pp. 1–11, 10.1109/AERO50100.2021.9438157.
- [3] Zuehlke, D., Henderson, T., Lovell, T.A., and Sizemore, A., “An End-to-End Process for Local Space Situational Awareness from Optical Observers,” 2020 IEEE/ION Position, Location and Navigation Symposium (PLANS), Apr. 2020, pp. 1547–1555, 10.1109/PLANS46316.2020.9109868.
- [4] Anderson, J., Anderson, A., Zuehlke, D., Canales, D., and Lovell, T.A., “Resident Space Object Identification in Arbitrary Space Images,” Paper AAS 23-179, AAS/AIAA Spaceflight Mechanics Meeting, Austin TX, 2023.
- [5] Pech, C.S., Lovell, T.A., Paraschos, I., Pavetto-Stewart, E., Bottero, L., Torres, A., and Walker, G., “A Refined Approach to Resident Object Identification in Unresolved Space Imagery,” Paper AAS 25-017, AAS Rocky Mountain Guidance, Navigation, and Control Conference, Breckenridge CO, 2025.
- [6] Hog E., Fabricius C., Makarov V.V., Urban S., Corbin T., Wycoff G., Bastian U., Schwekendiek P., Wicenc A., “The Tycho-2 Catalogue of the 2.5 Million Brightest Stars,” 2000.
- [7] Gaia ESA Archive, <https://gea.esac.esa.int/archive/> [retrieved Feb 2025].